Acta Crystallographica Section D
Biological Crystallography
ISSN 0907-4449

Crystallization and preliminary X-ray diffraction analysis of the NAD-dependent non-phosphorylating GAPDH of the hyperthermophilic archaeon *Thermoproteus tenax*

Nina A. Brunner,[a]* Dietmar A. Lang,[b]† Matthias Wilmanns[b] and Reinhard Hensel[a]

[a]FB 9 Mikrobiologie, Universität-GH Essen, Universitätsstrasse 5, D-45117 Essen, Germany, and [b]EMBL Outstation Hamburg, c/o DESY, Notkestrasse 85, D-22038 Hamburg, Germany

† Present address: Fresenius Medical Care AG, Medical Department, Else-Kroener-Strasse 1, 61352 Bad Homburg, Germany.

Correspondence e-mail: nina.brunner@uni-essen.de

Received 7 May 1999
Accepted 22 October 1999

Recombinant non-phosphorylating NAD^+-dependent glyceraldehyde-3-phosphate dehydrogenase (GAPN) of the hyperthermophilic crenarchaeote *Thermoproteus tenax* has been overexpressed, purified and crystallized using the hanging-drop vapour-diffusion technique. Crystals of different habits were obtained from several precipitant solutions (salts and polyethylene glycols). Preliminary X-ray analysis was performed with crystals grown in ammonium formate, which belonged to the primitive hexagonal space group *P*622, and had unit-cell parameters $a = b = 184.8$, $c = 133.0$ Å, $\gamma = 120^\circ$. Assuming a molecular weight of 55 kDa, a Matthews parameter of 3.3 $Å^3\ Da^{-1}$ is calculated assuming two molecules per asymmetric unit. The diffraction limit of these crystals is 2.5 Å resolution.

1. Introduction

The NAD^+-dependent non-phosphorylating glyceraldehyde-3-phosphate dehydrogenase (GAPN) of the hyperthermophilic archaeon *T. tenax* (optimal growth temperature 359 K; Zillig *et al.*, 1981) catalyses the irreversible oxidation of glyceraldehyde-3-phosphate to 3-phosphoglycerate and has recently been identified as an integral constituent of the catabolic Embden–Meyerhof–Parnas (EMP) pathway in this organism (Brunner *et al.*, 1998).

The enzyme is allosterically regulated by a variety of intermediates of sugar and energy metabolism, such as glucose-1-phosphate, fructose-6-phosphate, adenosine phosphates and nicotinamide adenine dinucleotides. Most effectors induce positive cooperativity of co-substrate binding, with Hill coefficients up to 1.9. Owing to the high allosteric potential and the irreversible mode of catalysis, GAPN of *T. tenax* is considered to be the main control point of glycolysis, thus governing the carbon flux through the pathway in response to growth conditions. As reported previously, the EMP pathway represents the main route for carbohydrate metabolism in *T. tenax* (Siebers *et al.*, 1997); however, it differs from the classical pathway in two respects: (i) a reversible PP_i-dependent phosphofructokinase (PP_i-PFK) replaces the commonly found enzyme couple fructose bisphosphatase/ATP-dependent PFK (Siebers *et al.*, 1998) and (ii) the two GAPDHs differ in cosubstrate specificity and phosphorylating capacity (Hensel *et al.*, 1987). In addition to GAPN, an $NADP^+$-dependent phosphorylating GAPDH predominantly occurs under anabolic conditions. Since the PFK cannot fulfil its common function as a key enzyme at the entrance of the pathway, the two GAPDHs are assumed to substitute for the lacking regulatory potential. This hypothesis has been supported both by biochemical and genetic data. While the activity of $NADP^+$-dependent phosphorylating GAPDH is determined by mRNA abundance in response to growth conditions, GAPN is constitutively expressed and controlled at protein level by several allosteric effectors, enabling the cell to immediately adapt carbohydrate metabolism to alterations of the intracellular milieu and substrate supply (Brunner & Hensel, in preparation).

Sequence analysis of GAPN from *T. tenax* revealed that the enzyme belongs to the aldehyde dehydrogenase superfamily (ALDH; E.C. 1.2.1.3) and shows the highest sequence similarities to the subgroup of non-phosphorylating GAPDHs (E.C. 1.2.1.8; Brunner *et al.*, 1998). A number of these enzymes have been characterized from plant cytosols, where they oxidize photosynthetically generated triosephosphates (Kelly & Gibbs, 1973; Iglesias & Losada, 1988), but they have also been isolated from non-photosynthetic organisms such as protists or heterotrophic bacteria, where they are assumed to regenerate reduction equivalents (Boyd *et al.*, 1995). Surprisingly, the enzymic properties of the *T. tenax* GAPN suggest a significantly different physiological context, adding new aspects to the structural and functional plasticity within the ALDH superfamily (Habenicht *et al.*, 1994). As crystallographic studies to date are limited to unspecific ALDH (Steinmetz *et al.*, 1997; Liu *et al.*, 1997) and betainaldehyde dehydrogenase (Johansson *et al.*, 1998), the solution of the crystal structure of GAPN of *T. tenax* should not only elucidate the structural basis of its allosteric regulation, but

Table 1
Crystallization conditions and crystal parameters of *T. tenax* GAPN.

Precipitant	Morphology	Resolution (Å)	Unit-cell parameters			
			$a = b$ (Å)	c (Å)	$\alpha = \beta$ (°)	γ (°)
1.25 *M* ammonium sulfate†	Bipyramidal	2.8	185.0	134.1	90	120
2.0 *M* sodium formate‡	Bipyramidal	2.5	186.3	133.4	90	120
6.5–9.5%(*w*/*v*) PEG 20000§	Bipyramidal	3.5	90.2	262.0	90	120

† 0.1 *M* sodium citrate pH 5.6 as buffer. ‡ 0.1 *M* sodium acetate pH 5.6 as buffer. § 0.1 *M* Tris–HCl pH 8.5 as buffer.

should also add to our knowledge about the structural diversification within the ALDH superfamily.

2. Expression and purification

The coding gene for GAPN of *T. tenax* was introduced into the vector pET 15b (Stratagene, La Jolla, USA) *via* two new restriction sites created by PCR amplification with the mutagenic primers 5′-GGTGTAGCCG-TAGGTATA**TCATGA**GGGCTG-3′ and 5′-CGTGGCCAAGGCGGGGG**GGATCC**-CGGCGGGG-3′ (restriction sites shown in bold). Recombinant *E. coli* BL21(DE3) was grown in Luria–Bertani medium containing 100 µg ampicillin per medium (Sambrook *et al.*, 1989). Overexpression of the GAPN protein was induced by adding isopropyl-β-D-thiogalactoside (1 m*M*) when the optical density at 600 nm reached 1.0. Cellular protein was extracted and heat-precipitated as described previously (Brunner *et al.*, 1998) and dialyzed overnight against buffer *A* (50 m*M* HEPES, 500 m*M* KCl, 5 m*M* dithiothreitol pH 7.5). After hydrophobic interaction chromatography on phenyl Sepharose Fast Flow (Pharmacia, Uppsala, Sweden), enzymatic activity was recovered using a gradient of 0–50% ethylene glycol in buffer *A*. Ethylene glycol was quantitatively removed by excessive dialysis against buffer *B* (10 m*M* Bis–Tris–propane, 300 m*M* KCl, 5 m*M* dithiothreitol pH 7.5) and subsequent gel filtration on Sephadex 200 (Pharmacia, Uppsala, Sweden). The homogeneity of the protein was confirmed by denaturing gel electrophoresis (Laemmli, 1970) followed by silver staining (Heukeshoven & Dernick, 1985).

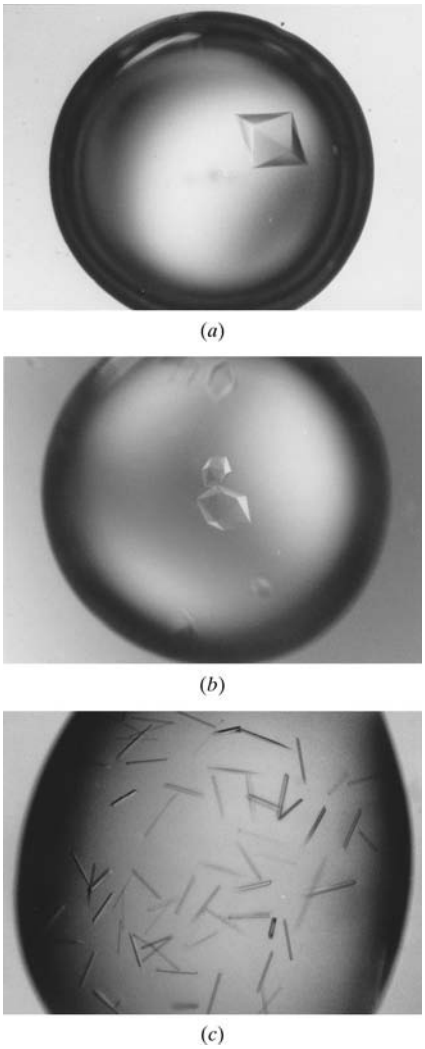

Figure 1
Photographs of crystals obtained by hanging-drop vapour diffusion in (*a*) 2 *M* ammonium sulfate, 0.1 *M* sodium citrate pH 5.6; (*b*) 2.0 *M* sodium formate, 0.1 *M* sodium acetate pH 5.6; (*c*) 8% PEG 8000, 0.1 *M* Tris–HCl pH 8.5. The crystal dimensions are 0.5 × 0.5 × 0.3 and 0.4 × 0.4 × 0.25 mm, respectively.

3. Crystallization

Homogeneous protein was concentrated by ultrafiltration (using Microcon 50; Amicon, Witten, Germany) to approximately 10 mg ml^{-1}. Crystallization conditions were screened in vapour-diffusion experiments using the protocol of Jancarik & Kim (1991), multi-factorial crystal screens from Hampton Research (Laguna Niguel, USA) and the footprinting setup modified by Stura & Wilson (1992). Crystallization drops consisting of 2 µl concentrated protein solution and 2 µl mother liquor were set up in hanging drops (McPherson, 1982) on siliconized cover slips over 500 µl reservoir solution. Crystallization was performed in Costar crystallization plates (Hampton Research, Laguna Niguel, USA) at 293 K. Within a few days, microcrystals of the protein were obtained from solutions containing several salts and polyethylene glycol (PEG) precipitants with different molecular weights over a broad pH range. The initial conditions were optimized by varying the concentrations of protein, precipitant and buffer system.

For preliminary X-ray analysis, some crystals were mounted in thin-walled glass capillaries and their diffraction properties were investigated by collecting test X-ray images on one of the protein crystallization synchrotron beamlines of the EMBL outstation at DESY, Hamburg. Cryo-conditions were established for one of the different crystal forms in order to collect a native data set.

4. Results and discussion

Crystals of different habits were grown from various salt and PEG solutions within a few days. Small crystals of bipyramidal shape were grown within 36 h from inorganic salt solutions used as precipitant at low pH (5.6). The change of the precipitant to a high molecular weight PEG (20 000) at higher pH (7–8) did not change the habit of the crystal (bipyramidal); however, when medium molecular weight PEGs (4000–8000) were used at pH 6.75–8, small rod-shaped crystals appeared within days. Some of the crystallization conditions were optimized in order to enlarge the crystal size to that suitable for preliminary X-ray analysis. The largest crystals, of dimensions up to 0.5 × 0.5 × 0.3 mm, were obtained from solutions using ammonium sulfate as precipitant (Fig. 1).

Preliminary X-ray analysis of crystals grown in medium molecular weight PEGs was impossible owing to their extreme sensitivity to radiation damage. Crystals grown either in sulfate, formate or PEG 20 000 could be tested. The *a* and *b* unit-cell dimensions of the crystals grown in the salt solutions are twice as long as those of the crystals grown in PEG (Table 1). The *c* unit-cell dimension behaves in the opposite way. The results of the preliminary analysis are summarized in Table 1.

Based on the preliminary X-ray analysis of the different crystal types, cryo-conditions were established for crystals grown from sodium formate by adding 20% glycerol to the mother liquor. A complete native data set was collected from one single crystal in 0.6° oscillation steps with a crystal-to-detector distance of 380 mm at 100 K on beamline X11 at the DESY. Processing and

Table 2
Native data set statistics of GAPN *T. tenax*.

Resolution (Å)	Unique reflections	Percentage observed (%)	R_{merge}† (%)	$I/\sigma(I)$
6.17	3387	97.5	3.9	29.8
4.89	3201	98.9	5.8	28.7
4.27	3151	99.3	6.0	28.2
3.88	3135	99.4	6.7	25.5
3.61	3101	99.6	6.7	23.3
3.39	3104	99.5	8.6	20.1
3.22	3101	99.7	11.2	15.7
3.08	3063	99.7	15.0	10.6
2.96	3082	99.9	20.4	7.5
2.86	3080	99.8	26.5	5.3
2.77	3051	99.9	35.7	4.2
2.69	3081	99.5	42.3	3.1
2.62	3052	99.0	50.2	2.5
2.56	3048	95.8	59.0	2.1
2.50	3048	92.4	67.2	1.5
Observations	46685	98.7	6.6	21.5

† $R_{merge} = \sum|I(k) - \langle I\rangle| / \sum I(k)$, where $I(k)$ is the value of the kth measurement of the intensity of a reflection, $\langle I\rangle$ is the mean value of the intensity of that reflection and the summation is over all measurements.

scaling of the data was performed using *DENZO*/*SCALEPACK* (Otwinowski & Minor, 1997; Table 2). The crystals belong to the primitive hexagonal space group *P*622, with refined unit-cell parameters $a = b = 184.8$, $c = 133.0$ Å, $\gamma = 120^\circ$. Assuming a molecular weight of 55 kDa for the protein (Brunner *et al.*, 1998) and two molecules per asymmetric unit, a Matthews parameter (Matthews, 1968) $V_M = 3.3$ Å^3 Da^{-1} can be calculated. However, a calculated self-rotation Patterson did not give an unambiguous non-crystallographically related peak solution. The structure elucidation will help to find an answer. These crystals diffracted to 2.5 Å resolution, but qualitatively the data set is only useful to 2.8 Å (beyond this, R_{merge} is greater than 35%).

Molecular-replacement calculations using three-dimensional models of aldehyde dehydrogenases as search models failed. Owing to the availibility of the protein expression for GAPN, we have started to overexpress the selenomethionine derivative of GAPDH. Therefore, the phase problem will be solved by a multiple anomalous diffraction (MAD) experiment.

References

Boyd, D. A., Cvitkovitch, D. G. & Hamilton, I. R. (1995). *J. Bacteriol.* **177**, 2622–2627.

Brunner, N. A., Brinkmann, H., Siebers, B. & Hensel, R. (1998). *J. Biol. Chem.* **273**, 6149–6156.

Habenicht, A., Hellmann, U. & Cerff, R. (1994). *J. Mol. Biol.* **237**, 165–171.

Hensel, R., Laumann, S., Lang, J., Heumann, H. & Lottspeich, F. (1987). *Eur. J. Biochem.* **170**, 325–333.

Heukeshoven, J. & Dernick, R. (1985). *Electrophoresis*, **6**, 103–112.

Iglesias, A. A. & Losada, M. (1988). *Arch. Biochem. Biophys.* **260**, 830–840.

Jancarik, J. & Kim, S.-H. (1991). *J. Appl. Cryst.* **24**, 409–411.

Johansson, K., El-Ahmad, M., Ramaswamy, S., Hjelmqvist, L., Jornvall, H. & Eklund, H. (1998). *Protein Sci.* **10**, 2106–2117.

Kelly, G. J. & Gibbs, M. (1973). *Plant Physiol.* **52**, 111–118.

Laemmli, U. K. (1970). *Nature (London)*, **277**, 680–685.

Liu, Z.-J., Sun, Y.-J., Rose, J., Chung, Y.-J., Hsaio, C.-D., Chang, W.-R., Perozich, J., Lindahl, R., Hempel, J. & Wang, B.-C. (1997). *Nature Struct. Biol.* **4**, 317–326.

McPherson, A. (1982). *Preparation and Analysis of Protein Crystals.* New York: John Wiley.

Matthews, B. W. (1968). *J. Mol. Biol.* **33**, 491–497.

Otwinowski, Z. & Minor, W. (1997). *Methods Enzymol.* **276**, 307–325.

Sambrook, J., Fritsch, E. F. & Maniatis, T. (1989). *Molecular Cloning: A Laboratory Manual*, 2nd ed. New York: Cold Spring Harbor Press.

Siebers, B., Klenk, H.-P. & Hensel, R. (1998). *J. Bacteriol.* **180**, 2137–2143.

Siebers, B., Wendisch, V. F. & Hensel, R. (1997). *Arch. Microbiol.* **168**, 120–127.

Steinmetz, C. G., Xie, P., Weiner, H. & Hurley, T. D. (1997). *Structure*, **5**, 701–711.

Stura, E. A. & Wilson, I. A. (1992). *Crystallization of Nucleic Acids and Proteins*, edited by A. Ducruix & R. Giegé, pp. 99–125. Oxford University Press.

Zillig, W., Stetter, K.-O., Schaefer, W., Janekovic, D., Wunderl, S., Holz, I. & Palm, P. (1981). *Zentralbl. Bakteriol. Hyg. C*, **2**, 205–227.